

ARTICLE OPEN



Hepatocyte TonEBP promotes metabolic stress-induced hepatic fibroinflammation involving transcriptional activation of ELR⁺ CXC chemokines

Jun Ho Lee^{1,2,3,14}, Hana Song^{4,14}, Eun Jin Yoo^{1,5,14}, Yeseul Jeong⁴, Seung Mi Ko⁴, Go Woon Shin¹, Gee Euhn Choi⁶, Youngheun Jee^{6,7,8}, Minhyeok Kang⁸, Jiwon Yang⁸, Sung-Pyo Hur⁹, Jong-Eun Park¹⁰, Yunkyoung Lee^{7,8,11}, Hye-Kyung Park¹², Ji-Hyun Yun⁴, Mi-Kyoung Jang⁴, Whaseon Lee-Kwon¹³, Hyug Moo Kwon¹³ and Soo Youn Choi^{4,7,8}

© The Author(s) 2026

Metabolic dysfunction-associated steatohepatitis (MASH), a progressive stage of metabolic dysfunction-associated steatotic liver disease (MASLD), is characterized by liver inflammation, fibrosis, and hepatocyte injury. Despite its clinical relevance, the molecular mechanisms linking metabolic stress to hepatic fibroinflammation remain poorly understood. In this study, we identify Tonicity-Responsive Enhancer-Binding Protein (TonEBP) as a key stress-responsive transcription factor that mediates the link between metabolic overload and liver inflammation in non-malignant hepatocytes. Using hepatocyte-specific TonEBP knockout (HKO) mice, we demonstrate that TonEBP deletion reduces liver injury, inflammation, and fibrosis in MASH and steatosis models. Mechanistically, TonEBP recruits nuclear factor- κ B (NF- κ B) to ELR⁺ CXC chemokine gene promoters, promoting neutrophil and macrophage recruitment. These findings underscore the hepatocyte-intrinsic TonEBP/NF- κ B axis as a critical driver of immune cell infiltration and fibroinflammation in MASLD progression, revealing its pivotal role in the pathophysiology of liver disease. By highlighting this axis, we provide new insight into the molecular mechanisms that govern the transition from steatosis to steatohepatitis, emphasizing the importance of TonEBP in regulating inflammatory pathways within hepatocytes.

Cell Death Discovery (2026)12:116; <https://doi.org/10.1038/s41420-026-02978-3>

INTRODUCTION

Metabolic dysfunction-associated steatohepatitis (MASH), a progressive form of metabolic dysfunction-associated steatotic liver disease (MASLD), is characterized by hepatic steatosis, inflammation, and fibrosis. The transition from MASLD to MASH significantly increases the risk of cirrhosis, liver failure, and hepatocellular carcinoma (HCC), making it a major global health concern [1, 2]. Despite advances in understanding the clinical features of MASH, the molecular mechanisms linking metabolic stress to hepatic fibroinflammation are multifactorial and remain incompletely understood. However, innate immunity plays a central role, with liver-resident macrophages (Kupffer cells) and recruited immune cells, such as macrophages and neutrophils, driving disease progression [3, 4].

Hepatocytes, the primary parenchymal cells of the liver, are essential for regulating hepatic metabolic functions and responding to metabolic stress [5, 6]. In conditions of chronic metabolic overload, such as obesity or lipotoxicity, hepatocytes become key initiators of liver inflammation and fibrosis by releasing proinflammatory cytokines and chemokines that recruit immune cells,

particularly neutrophils and macrophages [7–9]. These infiltrating immune cells further exacerbate the inflammatory and fibrotic environment, accelerating liver injury [9].

A critical regulator of cellular stress responses is tonicity-responsive enhancer-binding protein (TonEBP), also known as NFAT5. TonEBP is a stress-responsive transcription factor that integrates osmotic, metabolic, and inflammatory signals to regulate gene expression in a cell type- and context-dependent manner [10]. While TonEBP has been implicated in a variety of chronic conditions, including inflammation [11, 12], insulin resistance [13], adipose tissue dysfunction [14], and oncogenesis [15–17], its role in hepatocytes, especially under metabolic stress, remains poorly defined.

Previous studies have shown that TonEBP interacts with NF- κ B, a central transcription factor regulating proinflammatory gene expression. In macrophages, TonEBP enhances NF- κ B-dependent cytokine expression during inflammation [13, 18]. However, whether TonEBP regulates inflammatory pathways in hepatocytes during metabolic stress has yet to be determined.

¹Department of Biological Sciences, UNIST, Ulsan, Republic of Korea. ²Cancer Biology and Genetics Program, Sloan Kettering Institute, Memorial Sloan Kettering Cancer Center, New York, NY, USA. ³Graduate School of Stem Cell and Regenerative Biology, KAIST, Daejeon, Republic of Korea. ⁴Department of Biology, Jeju National University, Jeju, Republic of Korea. ⁵Department of Cell Biology, Albert Einstein College of Medicine, Bronx, NY, USA. ⁶Department of Veterinary Medicine, Jeju National University, Jeju, Republic of Korea. ⁷Center for Nutrition-Disease Research & Intervention System, Jeju National University, Jeju, Republic of Korea. ⁸Interdisciplinary Graduate Program in Advanced Convergence Technology & Science, Jeju National University, Jeju, Republic of Korea. ⁹Department of Marine Life Science, Jeju National University, Jeju, Republic of Korea. ¹⁰Department of Animal Biotechnology, Jeju National University, Jeju, Republic of Korea. ¹¹Department of Food Science and Nutrition, Jeju National University, Jeju, Republic of Korea. ¹²Research Institute for Basic Science, Jeju National University, Jeju, Republic of Korea. ¹³Graduate School of Health Science and Technology, UNIST, Ulsan, Republic of Korea. ¹⁴These authors contributed equally: Jun Ho Lee, Hana Song, Eun Jin Yoo. ✉email: hmkwon@unist.ac.kr; sychoi@jejunu.ac.kr

Received: 19 August 2025 Revised: 20 January 2026 Accepted: 16 February 2026

Published online: 26 February 2026

In this study, we investigate the role of TonEBP in hepatic inflammation and fibrosis in the context of MASLD and MASH. Using hepatocyte-specific TonEBP knockout (HKO) mice, we examine the effects of TonEBP deletion on liver injury, inflammation, and fibrosis in steatosis and steatohepatitis models. We show that TonEBP is essential for chemokine-driven neutrophil and macrophage infiltration, and that its interaction with NF- κ B regulates the transcriptional activation of ELR⁺ CXC chemokines. These findings highlight the TonEBP–NF- κ B axis as a critical mechanism in the progression of MASLD to MASH.

RESULTS

Hepatocyte TonEBP coordinates fibroinflammatory and metabolic gene programs under metabolic stress

To investigate the role of hepatocyte-intrinsic TonEBP in metabolic stress-driven fibroinflammation, we generated hepatocyte-specific TonEBP knockout (HKO) mice (Fig. S1) and applied two dietary models: methionine- and choline-deficient (MCD) and high-fat, high-carbohydrate (HFHC) diets. The MCD diet induces steatosis, inflammation, hepatocellular ballooning, cell death, and progressive fibrosis, closely reflecting advanced histological features of human MASH [19]. It is widely used for reproducible analysis of disease-related transcriptional changes and pathway-level responses, but does not induce obesity or insulin resistance. The HFHC diet, in contrast, produces milder yet progressive liver injury associated with obesity, insulin resistance, and fructose intake, more closely modeling the metabolic context of human MASLD/MASH [20, 21]. Using both models allowed us to assess the contribution of hepatocyte TonEBP under distinct metabolic stress conditions.

In MCD-fed mice, wild-type (WT) and HKO groups showed comparable weight loss (~40%) and food intake (Figs. 1A, B, and S2A). Steatosis and serum triglyceride levels were similar (Figs. 1C, D and S2B, C), but Sirius Red staining revealed markedly reduced fibrosis in HKO livers (Figs. 1E and S2D). Serum ALT, AST, and LDH were also significantly lower in HKO mice (Figs. 1F and S2E). Hepatic expression of *TonEBP* and 20 fibrosis-related genes linked to human MASH [22] was significantly decreased in HKO mice (Figs. 1G and S2F).

To explore transcriptional changes, we performed RNA-seq on liver tissue. Principal component analysis showed that HKO samples clustered with the control group fed a normal diet and were clearly separated from MCD-fed WT mice (Fig. 2A). Differential expression analysis identified 5,325 differentially expressed genes (DEGs) between WT-CD and WT-MCD, and 822 DEGs between WT-MCD and HKO-MCD (Fig. 2B). KEGG analysis revealed enrichment of fibrogenic and ECM-related pathways (“ECM–receptor interaction,” “PI3K–Akt signaling”) in WT-MCD, which were suppressed in HKO-MCD, while metabolic pathways downregulated by MCD were restored (Fig. S3A, B). GO enrichment analysis supported these findings (Fig. S4A–F). K-means clustering showed reduced expression of fibrosis-related clusters, including Cluster 5, in HKO livers (Figs. 2C–E and S5A, B). GSEA demonstrated downregulation of inflammatory and fibrotic pathways (“inflammatory response,” “TNF α signaling via NF- κ B,” “epithelial–mesenchymal transition”) and upregulation of metabolic programs (“oxidative phosphorylation,” “bile acid metabolism”) (Fig. S6A, B). Mapping mouse DEGs to human orthologs confirmed conserved suppression of inflammatory/fibrotic signatures and restoration of metabolic pathways in HKO livers (Figs. 2F, G and S7).

We next evaluated hepatocyte TonEBP in an obesity-associated setting using the HFHC model, which reflects Western dietary patterns high in cholesterol, saturated fats, and fructose [20, 21]. WT and HKO mice showed similar body weight, food intake, and water consumption during 16 weeks of feeding (Fig. 3A–C). HKO mice had significantly lower fasting glucose (Fig. 3D) and liver-to-

body weight ratios (Fig. 3E). Histology revealed reduced steatosis and fibrosis (Fig. 3F, G), with lower serum ALT, AST, and LDH (Fig. 3H). Fibrosis-related genes were downregulated (Fig. 3I).

These findings indicate that hepatocyte TonEBP is necessary for activation of inflammatory, fibrogenic, and metabolic stress-responsive programs in both lipotoxic and obesity-associated injury.

Hepatocyte TonEBP depletion attenuates hepatic inflammation across diverse metabolic stress models

Inflammation drives the progression from simple steatosis to MASH, fibrosis, and cirrhosis [23–26]. To determine the contribution of hepatocyte TonEBP, we examined inflammatory and immune-related gene expression in different metabolic stress models. In MCD-fed WT mice, chemokines (*Cxcl1*, *Cxcl2*, *Ccl2*), adhesion molecules (*Icam1*), and cytokines (*Tnfa*, *Il1b*) were strongly induced (Fig. S8A), matching the transcriptomic profiles of WT-MCD livers. This induction was significantly reduced in HKO mice (Fig. 4A). Similar suppression was seen in HFHC-fed HKO mice (Fig. 4B).

In the high-fat diet (HFD) model, which induces injury more gradually, HKO mice also showed reduced expression of these inflammatory markers after 14 weeks (Fig. 4C), without changes in body weight (Fig. 4D). Reduced hepatic inflammation correlated with improved systemic metabolic outcomes: lower fasting glucose and insulin, reduced HOMA-IR, and improved glucose tolerance (Fig. 4E–H). TonEBP deletion efficiency was confirmed by reduced hepatic *TonEBP* mRNA in HFD-fed HKO mice (Fig. 4I). These results demonstrate that hepatocyte TonEBP promotes hepatic inflammation in multiple metabolic stress settings and contributes to systemic insulin resistance.

Hepatocyte TonEBP promotes neutrophil and macrophage infiltration, in part by transcriptional activation of ELR⁺ CXC chemokines

To determine whether reduced *Mpo* and *F4/80* expression in HKO livers (Fig. 4A, B) reflected decreased immune cell infiltration, we performed histological analyses. IHC and IF revealed abundant MPO⁺ neutrophils and F4/80⁺ macrophages in WT livers under MCD and HFHC feeding, with a stronger response in MCD-fed mice (Fig. S9A, B). In HKO mice, infiltration was markedly reduced (Figs. 5A, B and S9A, B). Serum and hepatic levels of *Cxcl1* and *Cxcl2*, potent ELR⁺ CXC chemokines that attract neutrophils, as well as *Ccl2*, a chemokine that recruits macrophages, were also significantly lower in HKO mice (Figs. 4A–C and 5C).

We next tested whether TonEBP directly regulates chemokine expression. To this end, we treated primary human hepatocytes (PHHs) with palmitic acid (PA), a lipotoxic saturated fatty acid known to accumulate in metabolic liver disease [27, 28]. PHHs treated with PA showed dose-dependent induction of *CXCL8* (*IL-8*), *CXCL1*, and *CXCL2* within 3 h, sustained up to 9 h (Fig. 5D–E), along with increased TonEBP protein (Fig. 5F). *CCL2* transcripts were undetectable (Ct > 35), suggesting that hepatocytes preferentially express neutrophil-attracting ELR⁺ CXC chemokines in response to lipotoxic stress. Since monocytes and macrophages can express *CXCR1* and *CXCR2* under inflammatory conditions, ELR⁺ CXC chemokines may also contribute to macrophage recruitment [29, 30]. Based on this, we focused subsequent analyses on TonEBP-dependent regulation of ELR⁺ CXC chemokines. TonEBP knockdown using two independent siRNAs reduced TonEBP protein expression for up to 72 h (Fig. S10A) and significantly decreased PA-induced expression of *IL-8*, *CXCL1*, *CXCL2*, and *TonEBP* (Fig. 5G, H). PA also induced *TNFA*, confirming the proinflammatory effect of PA, which was attenuated by TonEBP knockdown (Fig. S10B–D). Similar reductions in these chemokine mRNA were observed in PA-treated AML-12 mouse hepatocytes and HepG2 cells, a human hepatoma line (Fig. S10E, F), indicating a conserved, hepatocyte-intrinsic role for TonEBP across species.

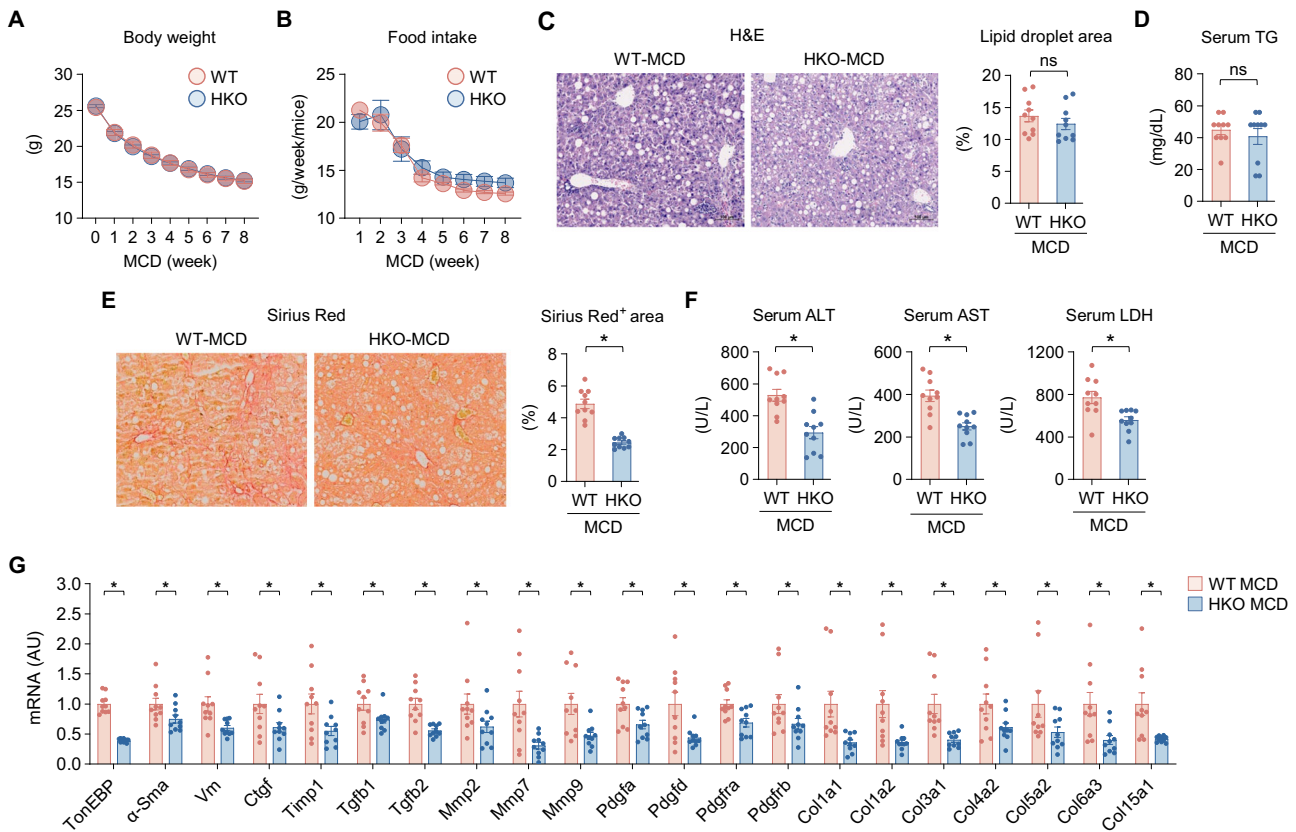


Fig. 1 Hepatocyte TonEBP depletion alleviates MCD-induced liver injury and fibrosis in mice. Male hepatocyte-specific TonEBP knockout (HKO) and wild-type (WT) mice (8 weeks old) were fed an MCD diet for 8 weeks ($n = 10$ per group). **A** Body weight (**A**) and food intake (**B**). **C** Representative H&E-stained liver sections and quantification of lipid droplet area. **D** Serum triglyceride levels. **E** Sirius Red staining and quantification of fibrotic area. **F** Serum ALT, AST, and LDH activities. **G** Hepatic expression of fibrosis-related genes determined by RT-qPCR. Data are presented as mean \pm SEM. Statistical significance was determined using an unpaired two-tailed Student's *t* test. $p < 0.05$ vs. WT; ns not significant.

siTon #1 was used in subsequent experiments. HepG2 cells, which showed consistent PA responses and high transfection efficiency, were used for mechanistic studies. TonEBP depletion also reduced secretion of IL-8, CXCL1, and CXCL2 (Fig. 5I), and conditioned medium from TonEBP-depleted cells showed diminished HL-60 migration (Figs. 5J and S11A). Neutralizing individual chemokines partially inhibited migration, with additive effects when combined with TonEBP knockdown (Fig. 5K). Conversely, adenoviral over-expression enhanced PA-induced chemokine expression (Fig. S11B, C).

We also examined TNF α and H₂O₂, which enhance NF- κ B activity and promote inflammatory gene expression in steatohepatitis [31, 32]. Both stimuli increased TonEBP and chemokine expression in PHHs (Fig. S12A–D), HepG2 (Fig. S13A–C), and AML-12 cells (Fig. S13D–F), and these effects were blocked by TonEBP knockdown. TonEBP promoter activity was also elevated (Fig. S13G). These data show that TonEBP promotes ELR⁺ CXC chemokine production under metabolic and inflammatory stress.

TonEBP is required for NF κ B recruitment to IL-8, CXCL1, and CXCL2 promoters

To determine whether TonEBP regulates IL-8, CXCL1, and CXCL2 transcription, we performed luciferase reporter assays using their proximal promoters in HepG2 cells (Fig. S14A). PA increased the promoter activity of IL-8, CXCL1, and CXCL2, which was reduced by TonEBP knockdown (Fig. 6A), and NF- κ B-driven reporter activity was decreased in TonEBP-deficient cells (Fig. S14B). Notably, these promoters do not contain a canonical TonEBP-binding motif (Fig. S14C). Given that NF- κ B is a key transcriptional

regulator of these genes [33–35] and that TonEBP has been shown to potentiate TNF α transcriptional activity in macrophages through its interaction with NF- κ B p65 [18], we investigated whether TonEBP facilitates NF- κ B-dependent transactivation of PA-induced IL-8, CXCL1, and CXCL2 in hepatocytes. Mutation of NF- κ B binding sites abolished PA-induced promoter activity (Figs. 6B and S14A). ChIP-qPCR confirmed increased TonEBP occupancy at these promoters after PA, TNF α , or H₂O₂ stimulation (Figs. 6C and S13C; S15A, B). TonEBP knockdown reduced PA-induced p65 recruitment (Fig. 6D), and co-immunoprecipitation revealed a PA-dependent TonEBP–p65 interaction (Figs. 6E and S15C). Similarly, p65 recruitment in response to TNF α or H₂O₂ was diminished in TonEBP-deficient cells (Fig. 6F, G), and mutation of the NF- κ B binding site abrogated promoter activation by both stimuli (Fig. 6H, I). We next examined the TonEBP–p65 interaction in vivo using liver extracts from WT and HKO mice fed a CD or an MCD diet. In WT livers, MCD feeding increased TonEBP protein levels without affecting total p65 levels, accompanied by enhanced co-precipitation of p65 with TonEBP, indicating increased complex formation (Fig. S15D–F). In contrast, this interaction was markedly attenuated in HKO mice, in which TonEBP induction was blunted (Fig. S15G, H). Reciprocal immunoprecipitation using p65 confirmed these findings, showing increased association of TonEBP with p65 in WT MCD-fed livers but not in HKO livers (Fig. S15G, H). Densitometric analyses normalized to the corresponding input signals further demonstrated that the fraction of p65 associated with TonEBP was increased under MCD-induced metabolic stress and abolished by hepatocyte-specific deletion of TonEBP (Fig. S15I).

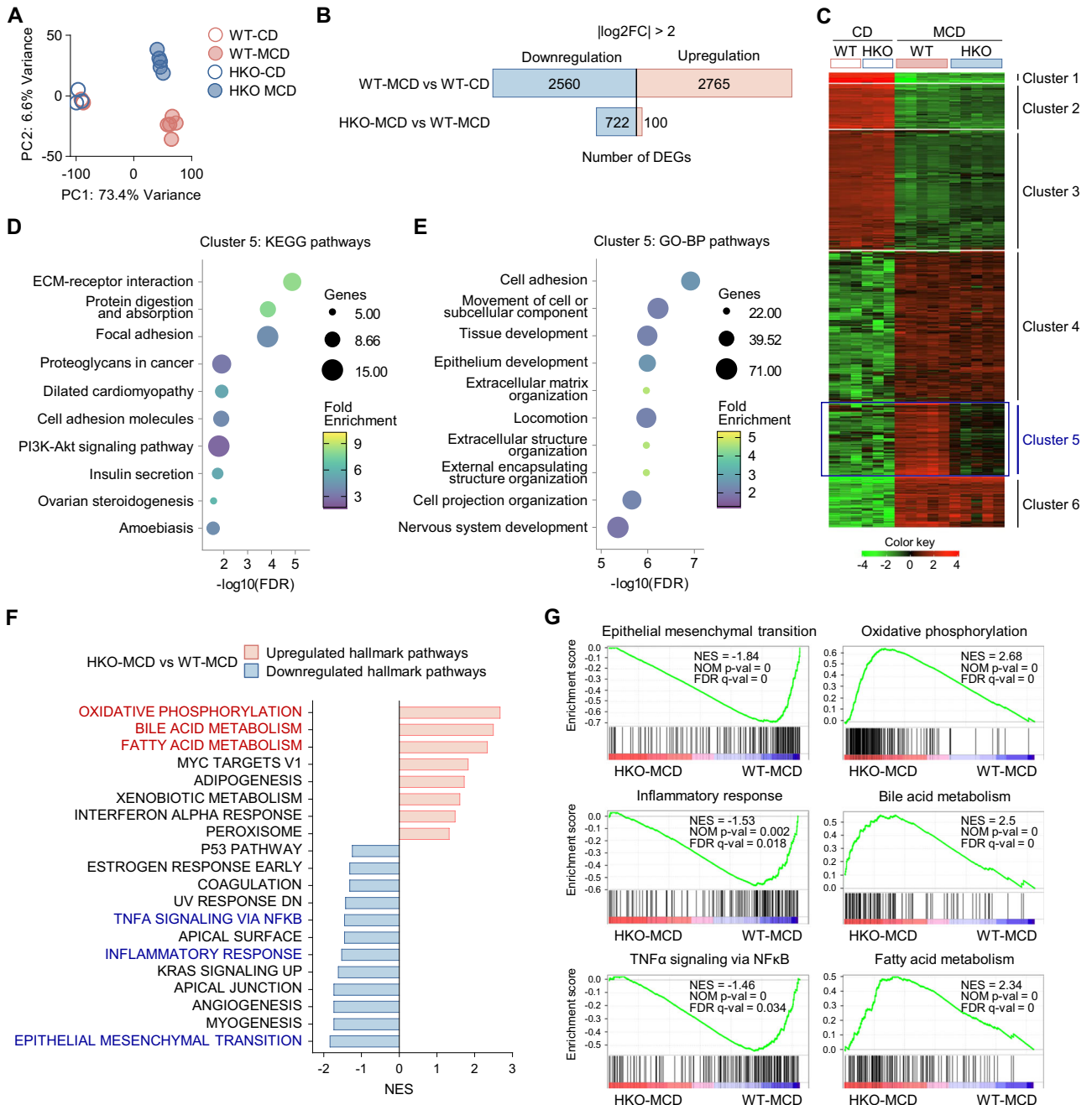


Fig. 2 Liver transcriptome analysis reveals reduced steatohepatitis-related gene expression in TonEBP-deficient mice. RNA-seq was performed on livers from male WT and HKO mice fed a control diet (CD, $n = 3$) or MCD diet ($n = 5$) for 8 weeks. **A** PCA plot. **B** Number of differentially expressed genes (DEGs) between groups identified by DESeq2 and edgeR ($|\log_2FC| > 2$, FDR < 0.05). **C** K-means clustering of the top 2000 variable genes. KEGG (**D**) and GO-BP (**E**) enrichment analyses for Cluster 5 genes. **F** GSEA normalized enrichment scores (NES) for HKO-MCD vs. WT-MCD livers. **G** Representative enrichment plots for selected pathways.

Disruption of the TonEBP–NF κ B interaction recapitulates TonEBP deficiency

To assess the functional significance of the TonEBP–NF- κ B interaction, we disrupted the complex using cerulenin, a known inhibitor of TonEBP–NF- κ B binding [18]. Co-immunoprecipitation confirmed that cerulenin impaired TonEBP–p65 interaction in HepG2 cells (Figs. 7A and S16A). Cerulenin treatment significantly reduced PA-induced *IL-8*, *CXCL1*, *CXCL2* (Fig. 7B), and *TNF α* (Fig. S16B) expression, and decreased promoter activity (Fig. 7C). Cerulenin also attenuated chemokine induction by *TNF α* and H_2O_2 (Fig. 7D, E). These effects mirrored those of TonEBP knockdown, confirming that the

TonEBP–NF- κ B complex is essential for maximal inflammatory gene activation in hepatocytes under metabolic stress. A schematic model summarizing our findings is presented in Fig. 7F, illustrating how hepatocyte TonEBP, through interaction with NF- κ B, promotes transcription of ELR $^+$ CXC chemokines, thereby driving immune cell infiltration, hepatic inflammation, and progression of steatohepatitis.

DISCUSSION

This study identifies hepatocyte TonEBP as a central transcriptional regulator that links metabolic stress to hepatic fibroinflammation

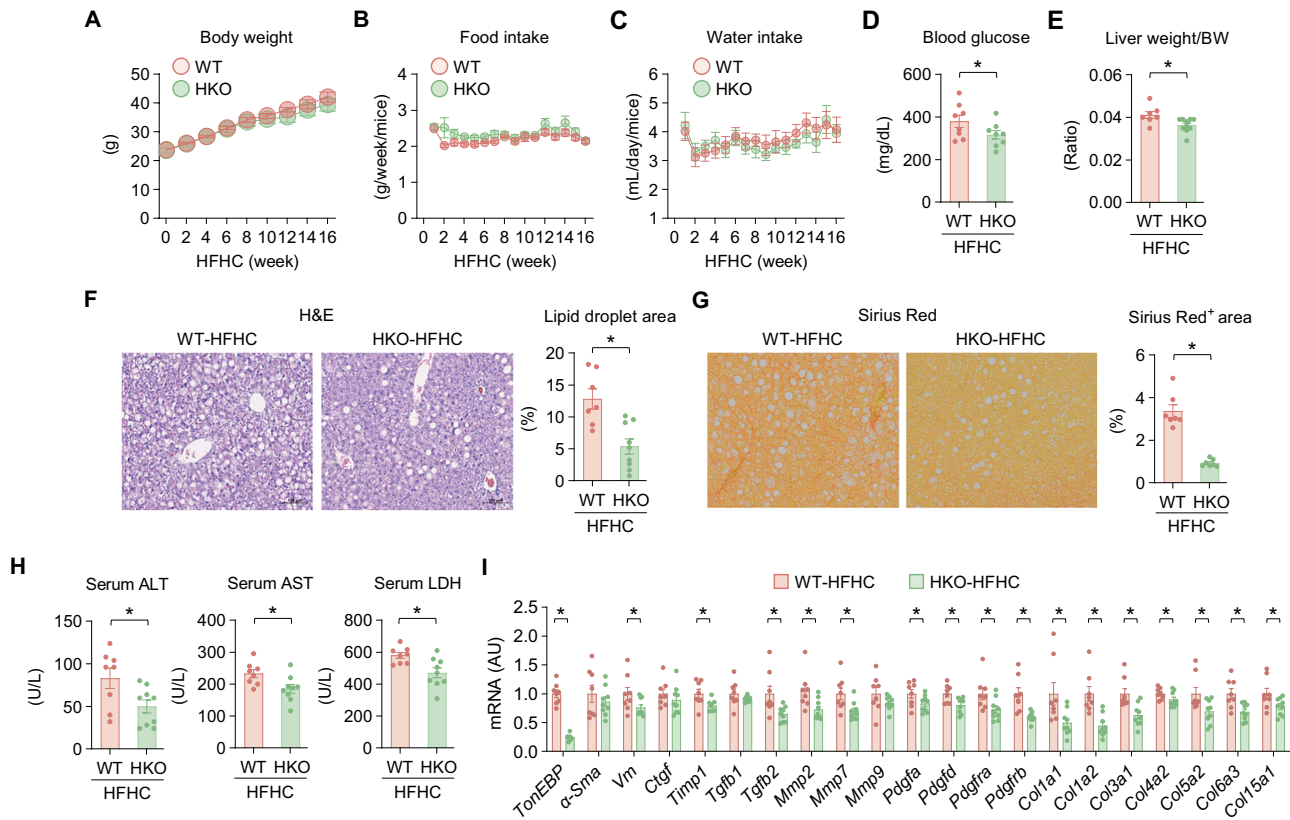


Fig. 3 Hepatocyte TonEBP deficiency attenuates liver injury and fibrosis in HFHC-fed mice. Male WT and HKO mice were fed an HFHC diet for 16 weeks ($n = 8$ per group). Body weight (A) food intake (B) water intake (C) fasting blood glucose (D) and liver-to-body weight ratio (E). F Representative H&E-stained sections and lipid droplet quantification. G Sirius Red staining and fibrotic area quantification. H Serum ALT, AST, and LDH activities. I Hepatic expression of fibrosis-related genes determined by RT-qPCR. Data are presented as mean \pm SEM. Statistical significance was determined using an unpaired two-tailed Student's t test. * $p < 0.05$ vs. WT.

through induction of ELR⁺ CXC chemokines, including *IL-8*, *CXCL1*, and *CXCL2*. These chemokines are potent neutrophil chemoattractants and can also recruit macrophages under inflammatory conditions. We show that TonEBP acts in hepatocytes by forming a complex with NF- κ B, enabling transcriptional activation of chemokine genes in response to lipotoxic, oxidative, and cytokine stress. This defines a hepatocyte-intrinsic mechanism by which metabolic stress drives immune cell infiltration and inflammation in metabolic liver diseases.

The transition from MASLD to MASH is characterized by persistent inflammation with infiltration of neutrophils and macrophages [24–26], which form crown-like structures associated with advanced fibrosis and worse outcomes [36, 37]. These cells exacerbate liver injury by releasing reactive oxygen species, proinflammatory cytokines, and extracellular traps, thereby sustaining a pro-fibrogenic milieu [3, 4, 38–40]. In our models, hepatocyte-specific TonEBP deletion reduced both neutrophil and macrophage accumulation, accompanied by suppression of chemokine expression and fibroinflammatory gene programs. This effect was observed in both lipotoxic (MCD) and obesity-associated (HFHC) models, indicating a conserved role for TonEBP in metabolic stress-induced hepatic inflammation.

Chronic liver inflammation reflects coordinated interactions among hepatocytes, Kupffer cells, hepatic stellate cells (HSCs), and sinusoidal endothelial cells [25, 41–43]. Under metabolic stress, hepatocytes release chemokines and danger signals that activate Kupffer cells and HSCs. Activated Kupffer cells secrete cytokines to amplify inflammation, while HSCs differentiate into myofibroblasts, leading to extracellular matrix deposition. Our findings place hepatocyte TonEBP at the upstream point of this network: its

deletion not only suppresses chemokine expression but also reduces immune cell infiltration, fibrosis, and hepatocellular injury, highlighting the pivotal intrinsic role of hepatocytes in shaping the liver's response to metabolic stress and inflammation. Notably, the protective effects of TonEBP deletion were consistently observed across multiple models of steatohepatitis, suggesting that this mechanism is conserved and broadly applicable, regardless of the specific metabolic or dietary challenge.

The ELR⁺ CXC chemokines—*IL-8*, *CXCL1*, and *CXCL2*—and *CCL2* are clinically relevant in both animal models and human MASH, closely associated with immune cell infiltration, disease activity, and fibrosis stage [44, 45]. Elevated serum *IL-8* and *CCL2* levels correlate with advanced fibrosis and poor prognosis in MASH patients [46]. *IL-8* is particularly elevated in chronic liver diseases, including cirrhosis, where it is linked to macrophage accumulation in the liver [30]. Consistently, *CXCR1* expression is upregulated in circulating monocytes from cirrhotic patients, underscoring the pathological importance of this chemokine signaling axis in disease progression [30]. Moreover, *IL-8* overexpression accelerates the progression from fatty liver to NASH [47], and the ELR⁺/ELR⁻ CXC chemokine ratio has been shown to modulate the severity of liver injury following ischemia/reperfusion [48], underscoring the broader regulatory influence of this chemokine network on hepatic inflammation and injury. In this context, our study identifies TonEBP as an upstream regulator of *IL-8*, *CXCL1*, and *CXCL2* in hepatocytes, providing mechanistic evidence that hepatocyte-derived TonEBP amplifies neutrophil-driven inflammation and fibrosis in MASH.

In mice, *Cxcl1* and *Cxcl2* function as *IL-8* analogs, mediating neutrophil recruitment, and TonEBP deletion reduces chemokine

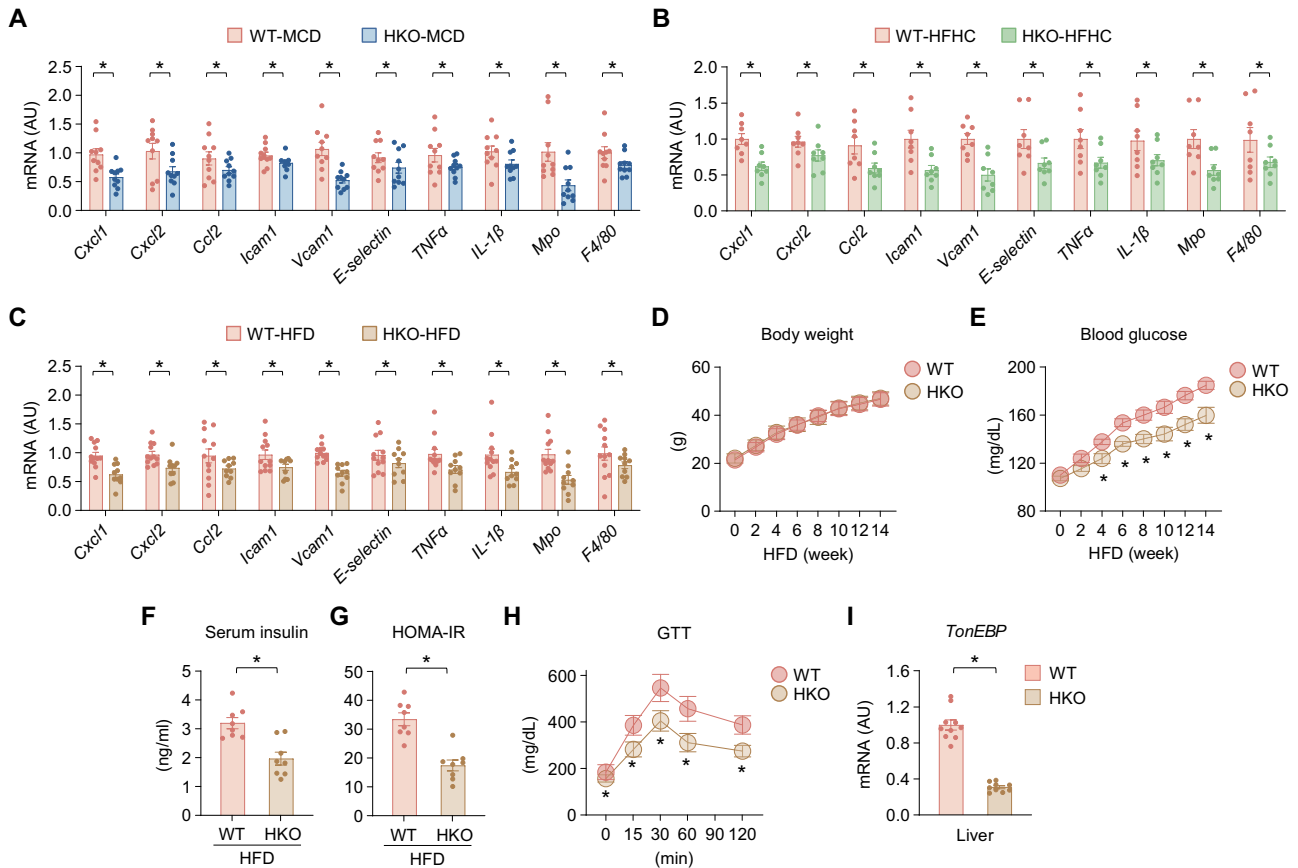


Fig. 4 Hepatocyte TonEBP depletion attenuates hepatic inflammation in metabolic stress models. Hepatic expression of inflammatory and fibrotic genes in WT and HKO mice fed an MCD diet for 8 weeks (A, $n = 10$) or an HFHC diet for 16 weeks (B, $n = 8$). In HFD-fed mice (14 weeks; WT, $n = 10$; HKO, $n = 9$): hepatic inflammatory/fibrotic gene expression (C) body weight (D) fasting blood glucose (E) serum insulin (F) HOMA-IR (G) glucose tolerance test (H) and hepatic TonEBP mRNA expression (I). Data are presented as mean \pm SEM. Statistical significance was determined using unpaired two-tailed Student's *t* test. * $p < 0.05$ vs. WT.

expression, neutrophil migration in vitro, and immune cell infiltration in vivo. Notably, TonEBP does not activate these promoters through its traditional DNA-binding motif but rather enhances transcription by facilitating NF- κ B p65 recruitment. Loss-of-function experiments and pharmacological disruption of the TonEBP–NF- κ B complex both impaired chemokine induction and neutrophil chemotaxis, demonstrating that under metabolic stress, TonEBP cooperates with NF- κ B in hepatocytes to amplify inflammatory signaling. This finding extends previous studies showing that TonEBP activates NF- κ B signaling in immune cells, demonstrating a similar cooperative effect in hepatocytes under metabolic stress.

Previous studies have implicated TonEBP in multiple pathological settings, including inflammation and metabolic diseases. TonEBP haploinsufficiency has been shown to alleviate hepatic inflammation in diabetic mice [1], and TonEBP promotes obesity-induced insulin resistance through epigenetic suppression of adipose tissue beiging [2]. In addition, TonEBP in myeloid cells has been identified as a driver of obesity-induced insulin resistance [3] and characterized as an immunometabolic stress protein [4]. These findings collectively underscore the broad involvement of TonEBP in metabolic inflammation. Our study extends this body of work by identifying a hepatocyte-intrinsic role of the TonEBP–NF- κ B axis in driving chemokine induction (CXCL1, CXCL2, IL-8) and immune cell recruitment under metabolic stress. This hepatocyte-specific mechanism provides a distinct perspective that complements prior studies centered on systemic, adipose, or myeloid contexts, highlighting a unique contribution of hepatocyte TonEBP to fibroinflammatory progression in MASH.

MASH is a multifactorial disease involving multiple hepatic cell types. In addition to hepatocytes, Kupffer cells, HSCs, and sinusoidal endothelial cells play critical roles in disease progression [49–51]. Although our study focused on hepatocyte-intrinsic mechanisms, the protective phenotype observed in hepatocyte-specific TonEBP knockout mice may also involve indirect effects on non-parenchymal cells. In support of this possibility, TonEBP depletion in hepatocytes was accompanied by reduced activation of HSC- and Kupffer cell-associated gene programs, suggesting that hepatocyte TonEBP influences intrahepatic crosstalk that amplifies fibroinflammation. Future studies will be required to systematically define the cell-type-specific functions of TonEBP and their relative contributions to MASH pathogenesis.

The combined use of the MCD and HFHC diet models provides complementary insight into the role of hepatocyte TonEBP in MASH. The MCD model recapitulates key histological features of human MASH, including steatosis, hepatocellular ballooning, lobular inflammation, and progressive fibrosis [19], making it particularly useful for examining transcriptional and pathway-level responses, despite its lack of metabolic features such as obesity and insulin resistance. In contrast, the HFHC model more closely reflects the metabolic milieu of human MASLD/MASH—including obesity and insulin resistance—although hepatic injury develops more gradually and less severely [20, 21]. The consistent protective effects observed with hepatocyte TonEBP depletion across both models strengthen the robustness of our findings and support their translational relevance.

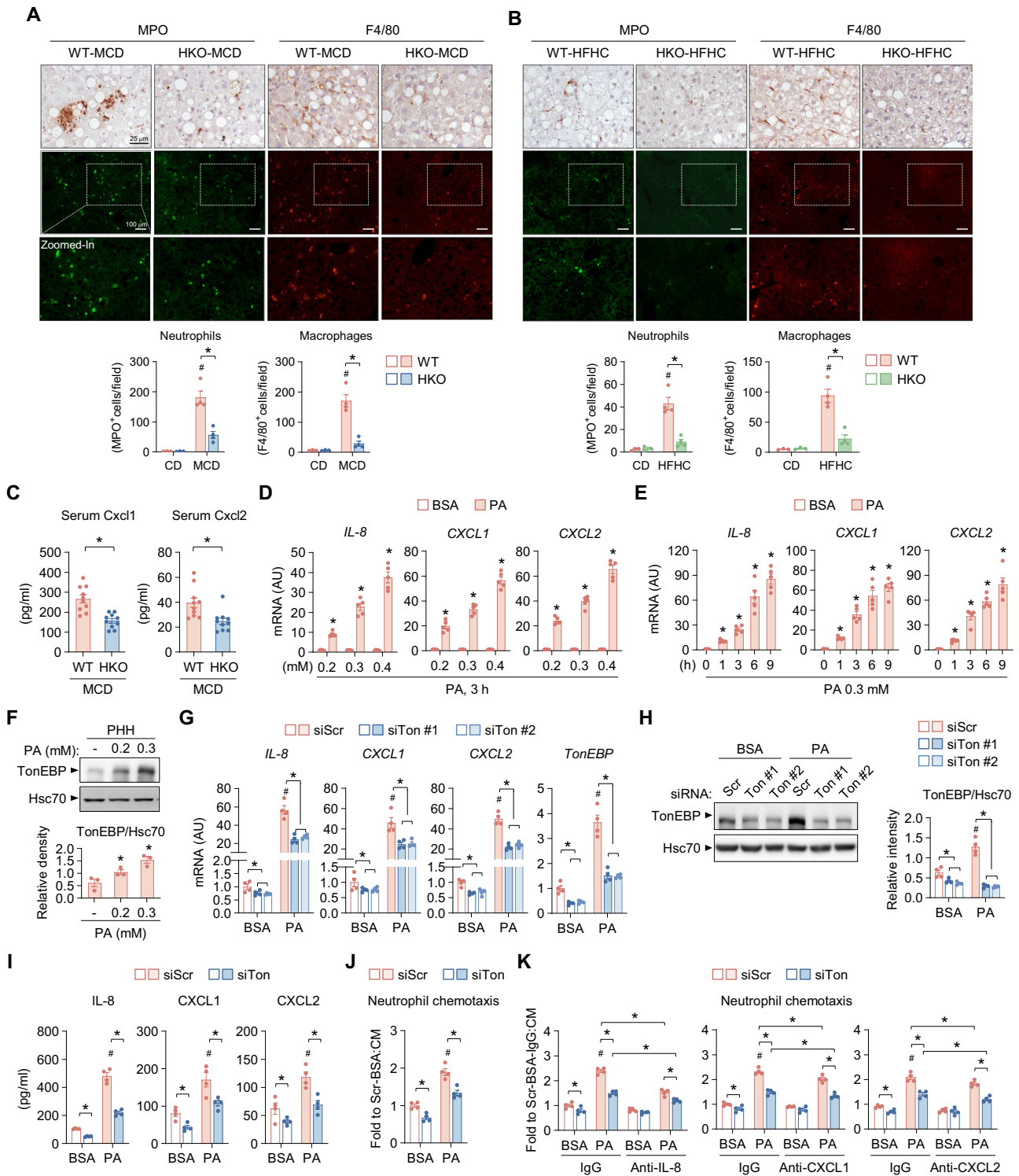


Fig. 5 Hepatocyte TonEBP promotes neutrophil and macrophage infiltration, in part by ELR⁺ CXC chemokine induction. Representative liver images from W) and HKO mice on a MCD diet (A) or a HFHC diet (B). IHC for MPO marks neutrophils, and IF for F4/80 marks macrophages. Quantification (cells/field) is shown below each set of images. Scale bars: IHC, 25 μ m; IF, 100 μ m. C Serum CXCL1 and CXCL2 levels in WT and HKO mice (MCD, $n = 10$). IL-8, CXCL1, and CXCL2 mRNA levels in primary human hepatocytes (PHHs) treated with BSA or palmitate (PA) at varying concentrations (D) or times (E). F Immunoblot of TonEBP protein in PHHs treated with BSA or PA; Hsc70 serves as a loading control, with densitometry (TonEBP/Hsc70) at bottom. G mRNA levels of IL-8, CXCL1, and CXCL2, and TonEBP after transfection with control (siScr) or TonEBP siRNAs (siTon #1/#2) followed by BSA or PA treatment. H Immunoblot analysis of TonEBP protein under the same conditions as in (G), with densitometric quantification at right. I Secreted chemokine proteins (IL-8, CXCL1, CXCL2) in conditioned medium (CM) from HepG2 cells after PA stimulation (BSA control). Neutrophil chemotaxis assays using hepatocyte-derived CM. Migration toward CM from BSA- or PA-treated cells (J). Chemotaxis after pretreatment of CM with isotype IgG or neutralizing antibodies against IL-8, CXCL1, or CXCL2 (K). Data are presented as mean \pm SEM (A–C) or SD (D–K) as indicated. Statistical significance was assessed by one-way ANOVA followed by Tukey's post hoc test for multiple comparisons. * $p < 0.05$; # $p < 0.05$ vs control.

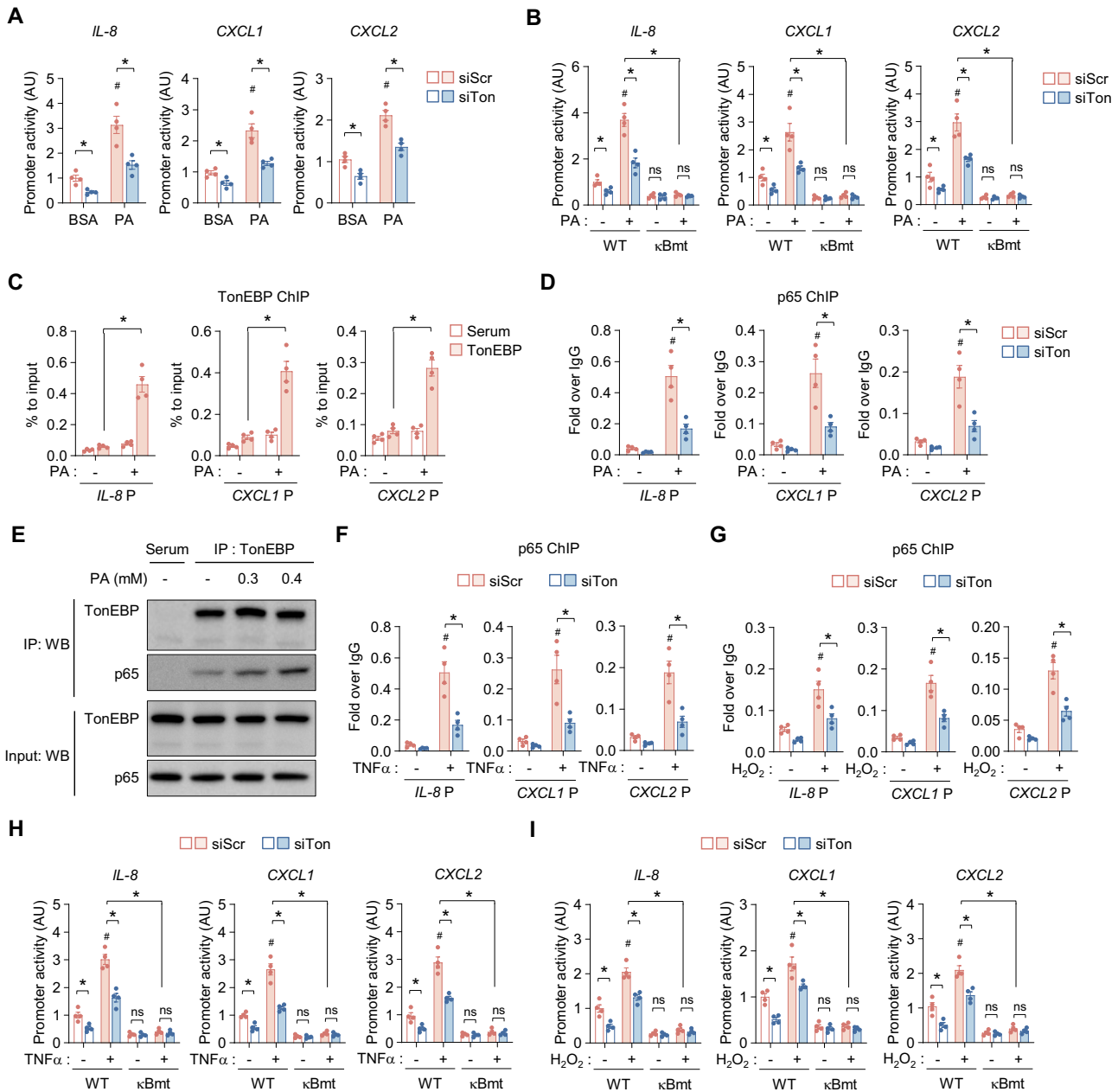


Fig. 6 TonEBP is required for NF- κ B recruitment to *IL-8*, *CXCL1*, and *CXCL2* promoters. Luciferase reporter assays in HepG2 cells with TonEBP knockdown using wild-type (WT) (A) or κ B mutant (κ Bmt) (B) promoter constructs for *IL-8*, *CXCL1*, and *CXCL2*, treated with BSA or PA. ChIP-qPCR analysis of TonEBP (C) and NF- κ B p65 (D) binding to κ B regions of the chemokine promoters after PA treatment. E Co-immunoprecipitation of TonEBP and p65 following PA treatment. p65 ChIP-qPCR after TNF α (F) or H₂O₂ (G) stimulation. Luciferase activity of WT and κ Bmt promoter constructs after TNF α (H) or H₂O₂ (I) treatment. Data are presented as mean \pm SD. Statistical significance was assessed by one-way ANOVA followed by Tukey's post hoc test for multiple comparisons. * p < 0.05 vs. WT; ns not significant.

Our study highlights the therapeutic potential of TonEBP as a target for metabolic liver diseases. TonEBP is known to promote pro-inflammatory programs in various tissues, including adipose tissue and macrophages [10]. Here, we extend its role to hepatocytes, identifying the TonEBP–NF- κ B complex as a key integrator of metabolic and inflammatory signals that converge on chemokine gene regulation. Inhibition of this axis reduces immune cell infiltration and fibrosis, supporting TonEBP as a viable target for neutrophil-dominant MASH phenotypes.

Despite these promising findings, several challenges remain. TonEBP is ubiquitously expressed and fulfills diverse physiological functions; therefore, systemic inhibition may lead to

undesirable side effects. More selective therapeutic strategies will be required to address this limitation. One approach is hepatocyte-specific delivery of siRNA using selective organ-targeting lipid nanoparticle systems, which enhance tissue specificity and reduce off-target effects [52]. Alternatively, selectively disrupting the TonEBP–NF- κ B interaction may attenuate its pro-inflammatory activity in hepatocytes while preserving its broader physiological roles. Such targeted strategies could improve both the safety and translational feasibility of TonEBP-directed therapies for MASH.

Several limitations should be considered. First, while we observed reduced neutrophil infiltration and chemokine

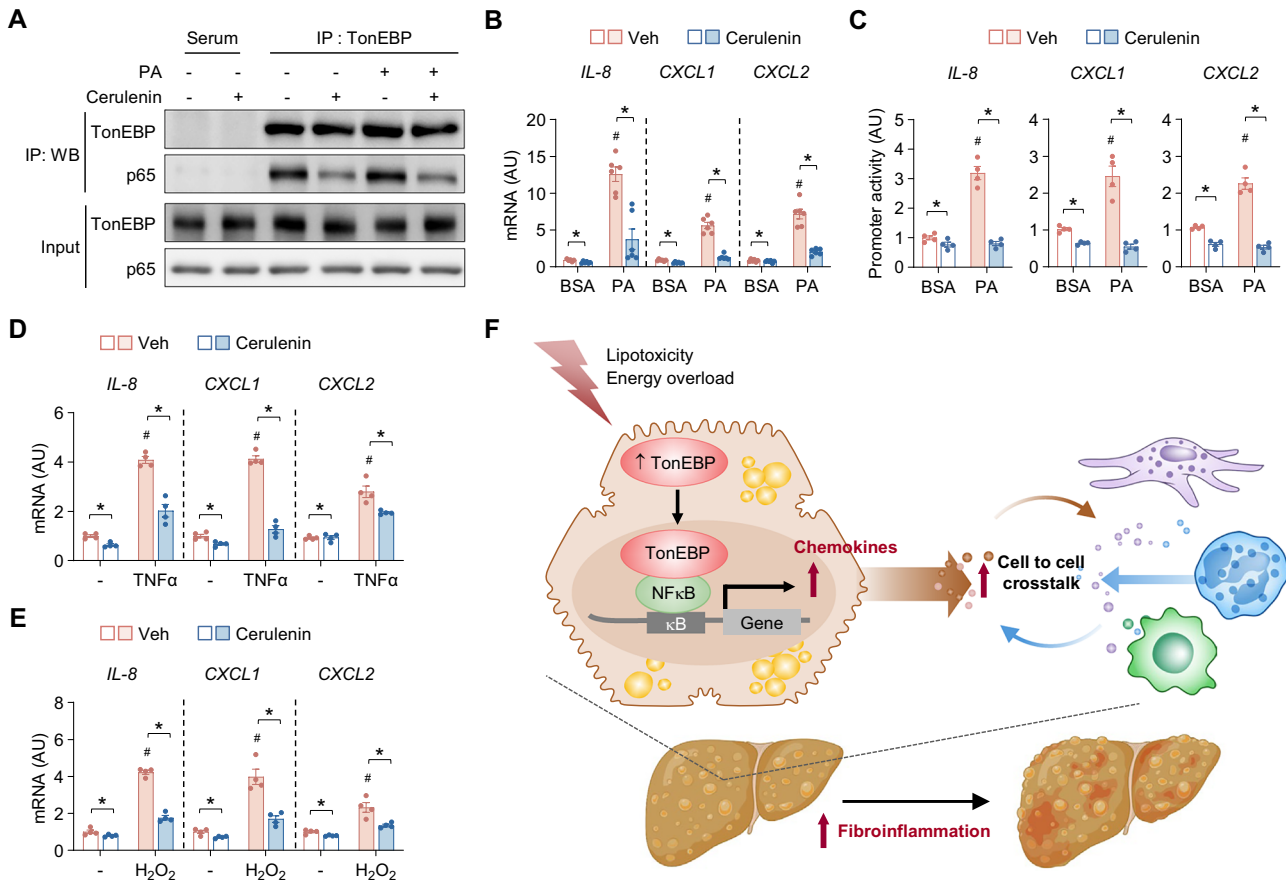


Fig. 7 Disruption of the TonEBP-NF- κ B interaction mimics TonEBP deficiency. HepG2 cells were pretreated with vehicle (Veh) or cerulenin (5 μ M) for 1 h, followed by treatment with BSA or palmitate (PA, 0.3 mM) for 3 h (A) or 9 h (B, C). Co-immunoprecipitation showing reduced TonEBP-p65 interaction in HepG2 cells pretreated with cerulenin (5 μ M) before PA stimulation (A). *IL-8*, *CXCL1*, and *CXCL2* mRNA levels after cerulenin and PA treatment (B). Luciferase activity of chemokine promoters (C). Chemokine mRNA levels after treatment with TNF α (10 ng/mL) (D) or H $_2$ O $_2$ (1 mM) (E) for 6 h in the presence or absence of cerulenin. F Proposed model illustrating how hepatocyte TonEBP, through NF- κ B interaction, promotes chemokine transcription, immune cell infiltration, and progression of steatohepatitis. Data are presented as mean \pm SD. Statistical significance was assessed by one-way ANOVA followed by Tukey's post hoc test for multiple comparisons. * p < 0.05 vs. vehicle; # p < 0.05 vs. control.

expression, the functional properties of infiltrating neutrophils, such as ROS production and NET formation, were not assessed. Second, species-specific differences in chemokine repertoires, notably the absence of IL-8 in mice, may limit the direct translation of our findings to humans. Third, although TonEBP deletion improved glucose metabolism in both HFHC and HFD models, insulin signaling in peripheral tissues was not evaluated. Finally, clinical validation using patient-derived samples is essential to confirm the relevance of our findings in human MASLD/MASH.

In conclusion, TonEBP emerges as a key hepatocyte-intrinsic regulator of chemokine-driven inflammation and fibrosis in metabolic liver diseases. Targeting the TonEBP-NF- κ B axis represents a promising therapeutic approach for treating MASH and other metabolically driven liver diseases.

MATERIALS AND METHODS

Animal studies

Male C57BL/6J mice (7–8 weeks) were used in all experiments. Hepatocyte-specific TonEBP knockout (HKO) mice were generated by crossing *TonEBP^{fl/fl}* mice [53] with *Alb-Cre* transgenic mice (Jackson Laboratory, Bar Harbor, ME) (Supplementary Fig. S1A). Hepatocyte-specific deletion was confirmed by assessing TonEBP protein levels in liver, kidney, spleen, and lung, demonstrating selective ablation in the

liver of *Cre⁺* mice (Fig. S17A). Under chow diet (CD) conditions, there were no differences in body weight, liver weight, or fasting glucose between *Cre⁺* and *Cre⁻* mice (Fig. S17B).

Age-matched littermates were assigned to experimental groups with body-weight balancing and fed one of the following diets obtained from Research Diets (New Brunswick, NJ), each paired with a model-specific control diet: (1) methionine- and choline-deficient (MCD) diet for 8 weeks; (2) high-fat, high-cholesterol (HFHC) diet for 16 weeks with drinking water supplemented with high-fructose corn syrup (42 g/L carbohydrates: 55% fructose and 45% sucrose; Sigma-Aldrich, St. Louis, MO); or (3) high-fat diet (HFD; 60% kcal from fat) for 14 weeks. Mice were euthanized for tissue collection, and liver injury, fibrosis, and inflammation were evaluated using histology, serum biochemical markers, and transcriptome analysis. No formal a priori statistical power calculation was performed. Sample sizes ($n = 8$ –10 per group) were determined based on effect sizes observed in our prior TonEBP studies and standard practice in dietary mouse models of MASH. Blinding was not performed; investigators were aware of group assignments during all experimental procedures and outcome assessments.

Histology and immunohistochemistry

Liver tissues were fixed in paraformaldehyde, embedded in paraffin, and stained with Hematoxylin and Eosin (H&E) and Sirius Red for histological evaluation of liver fibrosis and inflammation. Immunohistochemistry (IHC) for MPO and F4/80 (neutrophil and macrophage markers) was performed using standard protocols. Fluorescence images were captured using a Cytation 7 imaging system (NFC-2025-02-303179). Staining intensity and

positive cell counts were quantified using ImageJ software (<https://imagej.nih.gov/ij/>).

Glucose tolerance test

Following a 16-h fasting period, mice were injected intraperitoneally with glucose (2 g/kg). Blood samples were collected at various time points, and glucose levels were measured using a glucometer.

Immunoblot and chemokine analyses

Protein extraction and immunoblotting were performed using standard methods [54]. Protein concentrations were determined using the BCA assay (Pierce, Rockford, IL). Equal amounts of protein were separated by SDS-PAGE and probed with primary antibodies. HRP-conjugated secondary antibodies were used for detection via enhanced chemiluminescence (GE Healthcare, Buckinghamshire, UK). Primary antibodies used included anti-TonEBP [55], anti-NF- κ B p65 (Abcam, #ab16502), and anti-Hsc70 (Rockland, #200-301-A28, Limerick, PA, USA). The uncropped original western blots are provided in the “Uncropped WB data” file.

The levels of CXC chemokines Cxcl1 and Cxcl2 in mouse serum and cell culture media were quantified using ELISA kits (R&D Systems, Minneapolis, MN). IL-8 (CXCL8), CXCL1, and CXCL2 levels in human cell culture media were measured using Human Quantikine ELISA Kits (R&D Systems), following the manufacturer’s protocol.

Immunoprecipitation assay

Total cell lysates were prepared using RIPA buffer on ice. Lysates were incubated overnight at 4 °C with 5 μ g of antibody under rotary agitation. Protein A/G agarose beads (40 μ L, GE Healthcare) were then added and incubated for 2 h at 4 °C. After centrifugation, the beads were washed with RIPA buffer. Immunoprecipitated proteins were eluted by adding 40 μ L of sample buffer and boiling at 95 °C for 5 min. Eluted samples were analyzed by immunoblotting using anti-TonEBP and anti-NF- κ B p65 (Abcam, #ab16502) antibodies.

RNA-sequencing analysis

RNA was extracted from liver tissues and processed for RNA sequencing on the Illumina HiSeq platform. Differential expression analysis and Gene Set Enrichment Analysis (GSEA) were performed using StringTie (v2.1.3b) and iDEP (v2.01) [56].

Cell culture, transfection, and adenovirus infection

Primary human hepatocytes (PHHs; Lonza, Basel, Switzerland) were cultured on BioCoat Collagen I-coated plates (Corning, Steuben County, NY) and maintained in hepatocyte growth medium supplied by the manufacturer. HepG2 cells (HB-8065; ATCC, Manassas, VA) were maintained in Eagle’s MEM supplemented with 10% fetal bovine serum (FBS). AML12 cells (CRL-2254; ATCC) were cultured in DMEM containing 10% FBS, insulin (10 μ g/mL), transferrin (5.5 μ g/mL), selenium (5 ng/mL), and dexamethasone (40 ng/mL). HL-60 cells (CCL-240; ATCC) were cultured in RPMI-1640 medium supplemented with 10% FBS. All cells were maintained at 37 °C in a humidified incubator with 5% CO₂. The cell lines were not recently authenticated by STR profiling but were routinely tested for mycoplasma contamination and confirmed to be negative. For siRNA-mediated knock-down, PHHs, HepG2, and AML12 cells were transfected with scrambled siRNA (siScr) or gene-specific siRNAs (Integrated DNA Technologies, Coralville, IA) at equal concentrations using Lipofectamine RNAiMAX (Invitrogen, Carlsbad, CA) for 48 h. After transfection, cells were cultured in fresh medium, treated with the indicated chemicals, and processed for analysis. For overexpression experiments, HepG2 cells were infected with adenovirus expressing TonEBP (Ad-TonEBP) or control empty vector (Ad-EV) at a multiplicity of infection (MOI) of 50 for 24 h.

Palmitate (saturated fatty acid) treatment in vitro

Palmitate (PA) was conjugated to fatty acid-free bovine serum albumin (BSA) at a 6:1 molar ratio and added to the culture medium. Cells were treated with PA-BSA or 0.5% BSA alone as a vehicle control for the indicated durations and concentrations.

Real-time PCR

Total RNA was extracted using TRIzol® Reagent (Invitrogen), and cDNA was synthesized using M-MLV reverse transcriptase (Promega, Madison, WI).

Quantitative real-time PCR was performed using a CFX384 Real-Time PCR Detection System (Bio-Rad, Hercules, CA). Gene expression was normalized to *cyclophilin A* and calculated using the 2^{- $\Delta\Delta$ CT} method. Primer sequences are listed in Table S1.

Luciferase reporter assay

Cells were transfected with promoter-driven firefly luciferase constructs along with Renilla luciferase as an internal control. After 24 h, cells were treated as indicated, lysed in Passive Lysis Buffer, and analyzed using a dual-luciferase reporter assay system (Promega).

Chromatin immunoprecipitation (ChIP)-qPCR

HepG2 cells were treated as indicated. ChIP assays were performed using a commercial kit (Millipore, Bedford, MA). Cells were crosslinked with 1% formaldehyde, quenched with glycine, washed, and lysed in SDS lysis buffer. Chromatin was sonicated using a Bioruptor KRB-01 (BMS, Tokyo, Japan) to generate 400–1000 bp DNA fragments. Immunoprecipitation was carried out overnight at 4 °C using anti-TonEBP serum, anti-NF- κ B p65 antibody (#510500, Thermo Fisher Scientific), normal rabbit serum, or normal rabbit IgG (ab171870, Abcam). DNA was purified using the QIAquick PCR Purification Kit (QIAGEN, Redwood, CA) and analyzed by qPCR. Primer sequences are listed in Table S1.

Statistical analysis

Data are presented as means \pm standard deviation (SD) or standard error of the mean (SEM), as indicated. For comparisons between two groups, an unpaired two-tailed Student’s t-test was used. For comparisons involving more than two groups, one-way ANOVA followed by Tukey’s post hoc test was applied. Statistical significance was defined as $p < 0.05$. Analyses were performed using GraphPad Prism 10.0 (GraphPad Software, San Diego, CA).

DATA AVAILABILITY

All data supporting the conclusions in the paper are provided in the main text or the supplementary materials. Detailed datasets regarding RNA sequencing are available from the corresponding author upon reasonable request.

REFERENCES

1. Younossi Z, Anstee QM, Marietti M, Hardy T, Henry L, Eslam M, et al. Global burden of NAFLD and NASH: trends, predictions, risk factors and prevention. *Nat Rev Gastroenterol Hepatol*. 2018;15:111–20.
2. Babu AF, Palomurto S, Kärjälä V, Käkelä P, Lehtonen M, Hanhineva K, et al. Metabolic signatures of metabolic dysfunction-associated steatotic liver disease in severely obese patients. *Dig Liver Dis*. 2024;56:2103–10.
3. Kazankov K, Jørgensen SMD, Thomsen KL, Møller HJ, Vilstrup H, George J, et al. The role of macrophages in nonalcoholic fatty liver disease and nonalcoholic steatohepatitis. *Nat Rev Gastroenterol Hepatol*. 2019;16:145–59.
4. Hwang S, Yun H, Moon S, Cho YE, Gao B. Role of neutrophils in the pathogenesis of nonalcoholic steatohepatitis. *Front Endocrinol*. 2021;12:751802.
5. Meex RCR, Watt MJ. Hepatokines: linking nonalcoholic fatty liver disease and insulin resistance. *Nat Rev Endocrinol*. 2017;13:509–20.
6. Stefan N, Schick F, Birkenfeld AL, Häring HU, White MF. The role of hepatokines in NAFLD. *Cell Metab*. 2023;35:236–52.
7. Wang X, Zheng Z, Caviglia JM, Corey KE, Herfel TM, Cai B, et al. Hepatocyte TAZ/WWTR1 promotes inflammation and fibrosis in nonalcoholic steatohepatitis. *Cell Metab*. 2016;24:848–62.
8. Zhu C, Kim K, Wang X, Bartolome A, Salomao M, Dongiovanni P, et al. Hepatocyte notch activation induces liver fibrosis in nonalcoholic steatohepatitis. *Sci Transl Med*. 2018;10:eaat0344.
9. Schwabe RF, Tabas I, Pajvani UB. Mechanisms of fibrosis development in non-alcoholic steatohepatitis. *Gastroenterology*. 2020;158:1913–28.
10. Choi SY, Lee-Kwon W, Kwon HM. The evolving role of TonEBP as an immunometabolic stress protein. *Nat Rev Nephrol*. 2020;16:352–64.
11. Yoo EJ, Oh KH, Piao H, Kang HJ, Jeong GW, Park H, et al. Macrophage transcription factor TonEBP promotes systemic lupus erythematosus and kidney injury via damage-induced signaling pathways. *Kidney Int*. 2023;104:163–80.
12. Li M, Kim YM, Koh JH, Park J, Kwon HM, Park JH, et al. Serum amyloid A expression in liver promotes synovial macrophage activation and chronic arthritis via NFAT5. *J Clin Investig*. 2024;134:e167835.
13. Lee HH, Jeong GW, Ye BJ, Yoo EJ, Son KS, Kim DK, et al. TonEBP in myeloid cells promotes obesity-induced insulin resistance and inflammation through adipose tissue remodeling. *Diabetes*. 2022;71:2557–71.

14. Lee HH, Jeong GW, Ye BJ, Yoo EJ, Son KS, Kim DK, et al. TonEBP/NFAT5 promotes obesity and insulin resistance by epigenetic suppression of white adipose tissue beiging. *Nat Commun.* 2019;10:3536.
15. Choi SY. The roles of TonEBP in the DNA damage response: from DNA damage bypass to R-loop resolution. *DNA Repair.* 2024;140:103697.
16. Lee JH, Suh JH, Choi SY, Kang HJ, Lee HH, Ye BJ, et al. Tonicity-responsive enhancer-binding protein promotes hepatocellular carcinogenesis, recurrence and metastasis. *Gut.* 2019;68:347–58.
17. Lee JH, Suh JH, Kang HJ, Choi SY, Jung SW, Lee-Kwon W, et al. Tonicity-responsive enhancer-binding protein promotes stemness of liver cancer and cisplatin resistance. *EBioMedicine.* 2020;58:102926.
18. Lee HH, Sanada S, An SM, Ye BJ, Lee JH, Seo YK, et al. LPS-induced NFκB enhanceosome requires TonEBP/NFAT5 without DNA binding. *Sci Rep.* 2016;6:24921.
19. Machado MV, Michelotti GA, Xie G, Almeida PT, Boursier J, Bohnic B, et al. Mouse models of diet-induced nonalcoholic steatohepatitis reproduce the heterogeneity of the human disease. *PLoS ONE.* 2015;10:e0127991.
20. Vacca M, Kamzolas I, Harder LM, Andreassen M, Eriksen MB, Borrebaek J, et al. An unbiased ranking of murine dietary models based on their proximity to human metabolic dysfunction-associated steatotic liver disease (MASLD). *Nat Metab.* 2024;6:1178–96.
21. Jensen T, Abdelmalek MF, Sullivan S, Nadeau KJ, Green M, Roncal C, et al. Fructose and sugar: a major mediator of non-alcoholic fatty liver disease. *J Hepatol.* 2018;68:1063–75.
22. Hwang S, He Y, Xiang X, Seo W, Kim SJ, Ma J, et al. Interleukin-22 ameliorates neutrophil-driven nonalcoholic steatohepatitis through multiple targets. *Hepatology.* 2020;72:412–29.
23. Park I, Kim N, Lee S, Park K, Son MY, Cho HS, et al. Characterization of signature trends across the spectrum of non-alcoholic fatty liver disease using deep learning method. *Life Sci.* 2023;314:121195.
24. Huby T, Gautier EL. Immune cell-mediated features of non-alcoholic steatohepatitis. *Nat Rev Immunol.* 2022;22:429–43.
25. Peiseler M, Schwabe R, Hampe J, Kubes P, Heikenwälder M, Tacke F. Immune mechanisms linking metabolic injury to inflammation and fibrosis in fatty liver disease—novel insights into cellular communication circuits. *J Hepatol.* 2022;77:1136–60.
26. Hammerich L, Tacke F. Hepatic inflammatory responses in liver fibrosis. *Nat Rev Gastroenterol Hepatol.* 2023;20:633–46.
27. Joshi-Barve S, Barve SS, Amancherla K, Gobjeshvili L, Hill D, Cave M, et al. Palmitic acid induces production of proinflammatory cytokine interleukin-8 from hepatocytes. *Hepatology.* 2007;46:823–30.
28. Bence KK, Birnbaum MJ. Metabolic drivers of non-alcoholic fatty liver disease. *Mol Metab.* 2021;50:101143.
29. Rigamonti E, Fontaine C, Lefebvre B, Duhem C, Lefebvre P, Marx N, et al. Induction of CXCR2 receptor by peroxisome proliferator-activated receptor gamma in human macrophages. *Arterioscler Thromb Vasc Biol.* 2008;28:932–9.
30. Zimmermann HW, Seidler S, Gassler N, Nattermann J, Luedde T, Trautwein C, et al. Interleukin-8 is activated in patients with chronic liver diseases and associated with hepatic macrophage accumulation in human liver fibrosis. *PLoS ONE.* 2011;6:e21381.
31. Dong W, Simeonova PP, Gallucci R, Matheson J, Fannin R, Montuschi P, et al. Cytokine expression in hepatocytes: role of oxidant stress. *J Interferon Cytokine Res.* 1998;18:629–38.
32. Fromenty B, Roden M. Mitochondrial alterations in fatty liver diseases. *J Hepatol.* 2023;78:415–29.
33. Elliott CL, Allport VC, Loudon JA, Wu GD, Bennett PR. Nuclear factor-kappa B is essential for up-regulation of interleukin-8 expression in human amnion and cervical epithelial cells. *Mol Hum Reprod.* 2001;7:787–90.
34. Wood LD, Farmer AA, Richmond A. HMGI(Y) and Sp1 in addition to NF-kappa B regulate transcription of the MGSA/GRO alpha gene. *Nucleic Acids Res.* 1995;23:4210–9.
35. Wu Z, Neufeld H, Torlakovic E, Xiao W. Uev1A-Ubc13 promotes colorectal cancer metastasis through regulating CXCL1 expression via NF-κB activation. *Oncotarget.* 2018;9:15952–67.
36. Itoh M, Kato H, Suganami T, Konuma K, Marumoto Y, Terai S, et al. Hepatic crown-like structure: a unique histological feature in non-alcoholic steatohepatitis in mice and humans. *PLoS ONE.* 2013;8:e82163.
37. Fan M, Song E, Zhang Y, Zhang P, Huang B, Yan K, et al. Metabolic dysfunction-associated steatohepatitis detected by neutrophilic crown-like structures in morbidly obese patients: a multicenter and clinicopathological study. *Research.* 2024;7:0382.
38. Fabre T, Barron AMS, Christensen SM, Asano S, Bound K, Lech MP, et al. Identification of a broadly fibrogenic macrophage subset induced by type 3 inflammation. *Sci Immunol.* 2023;8:eadd8945.
39. Baragetti A, Da Dalt L, Moregola A, Svecla M, Terenghi O, Mattavelli E, et al. Neutrophil aging exacerbates high-fat diet-induced metabolic alterations. *Metabolism.* 2023;144:155576.
40. Liu K, Wang FS, Xu R. Neutrophils in liver diseases: pathogenesis and therapeutic targets. *Cell Mol Immunol.* 2021;18:38–44.
41. Kostallari E, Schwabe RF, Guillot A. Inflammation and immunity in liver homeostasis and disease: a nexus of hepatocytes, nonparenchymal cells and immune cells. *Cell Mol Immunol.* 2025;22:1205–25.
42. Ge C, Tan J, Dai X, Kuang Q, Zhong S, Lai L, et al. Hepatocyte phosphatase DUSP22 mitigates NASH-HCC progression by targeting FAK. *Nat Commun.* 2022;13:5945.
43. Loft A, Alfaro AJ, Schmidt SF, Pedersen FB, Terkelsen MK, Puglia M, et al. Liver-fibrosis-activated transcriptional networks govern hepatocyte reprogramming and intra-hepatic communication. *Cell Metab.* 2021;33:1685–700.e9.
44. Poulsen KL, Cajigas-Du Ross CK, Chaney JK, Nagy LE. Role of the chemokine system in liver fibrosis: a narrative review. *Dig Med Res.* 2022;5:30.
45. Ullah A, Ud Din A, Ding W, Shi Z, Pervaz S, Shen B. CXCL chemokines influence immune surveillance in obesity and obesity-related diseases: type 2 diabetes and nonalcoholic fatty liver disease. *Rev Endocr Metab Disord.* 2023;24:611–31.
46. Glass O, Henao R, Patel K, Guy CD, Gruss HJ, Syn WK, et al. Serum interleukin-8, osteopontin, and monocyte chemoattractant protein 1 are associated with hepatic fibrosis in patients with nonalcoholic fatty liver disease. *Hepatol Commun.* 2018;2:1344–55.
47. Cho YE, Kim Y, Kim SJ, Lee H, Hwang S. Overexpression of interleukin-8 promotes the progression of fatty liver to nonalcoholic steatohepatitis in mice. *Int J Mol Sci.* 2023;24:15489.
48. Colletti LM, Green ME, Burdick MD, Strieter RM. The ratio of ELR⁺ to ELR⁻ CXCL chemokines affects lung and liver injury following hepatic ischemia/ reperfusion in the rat. *Hepatology.* 2000;31:435–45.
49. Lanthier N. Targeting kupffer cells in non-alcoholic fatty liver disease/non-alcoholic steatohepatitis: why and how? *World J Hepatol.* 2015;7:2184–8.
50. Kisseleva T, Ganguly S, Murad R, Wang A, Brenner DA. Regulation of hepatic stellate cell phenotypes in metabolic dysfunction-associated steatohepatitis. *Gastroenterology.* 2025;169:797–812.
51. Miyao M, Kotani H, Ishida T, Kawai C, Manabe S, Abiru H, et al. Pivotal role of liver sinusoidal endothelial cells in NAFLD/NASH progression. *Lab Invest.* 2015;95:1130–44.
52. Wang X, Liu S, Sun Y, Yu X, Lee SM, Cheng Q, et al. Preparation of selective organ-targeting (SORT) lipid nanoparticles (LNPs) using multiple technical methods for tissue-specific mRNA delivery. *Nat Protoc.* 2023;18:265–91.
53. Küper C, Beck FX, Neuhofer W. Generation of a conditional knockout allele for the NFAT5 gene in mice. *Front Physiol.* 2015;5:507.
54. Mahmood T, Yang PC. Western blot: technique, theory, and troubleshooting. *N Am J Med Sci.* 2012;4:429–34.
55. Miyakawa H, Woo SK, Dahl SC, Handler JS, Kwon HM. Tonicity-responsive enhancer binding protein, a rel-like protein that stimulates transcription in response to hypertonicity. *Proc Natl Acad Sci USA.* 1999;96:2538–42.
56. Ge SX, Son EW, Yao R. iDEP: an integrated web application for differential expression and pathway analysis of RNA-Seq data. *BMC Bioinform.* 2018;19:534.

AUTHOR CONTRIBUTIONS

Jun Ho Lee, Hana Song, and Eun Jin Yoo contributed equally to writing the original draft, review and editing, conceptualization, investigation, data curation, validation, and visualization. Yeseul Jeong, Seung Mi Ko contributed to visualization, validation, and investigation. Go Woon Shin, Ji-Hyun Yun, and Mi-Kyoung Jang performed investigations and formal analysis. Gee Euhn Choi, Youngheun Jee, Minhyeok Kang, Jiwon Yang, Sung-Pyo Hur, Jong-Eun Park, Yunkyoung Lee, Hye-Kyung Park, and Whaseon Lee-Kwon provided resources and methodology. Hyug Moo Kwon and Soo Youn Choi supervised the project, reviewed and edited the manuscript, and secured funding. All authors read and approved the final manuscript.

FUNDING

This work was supported by the National Research Foundation of Korea (NRF) funded by the Korean government (MSIT); Grant Nos. RS-2023-NR076466, RS-2024-NR00416052, RS-2025-00514468) and the Ministry of Education (MOE) (2019R1A6A1A10072987). This research was also supported by the Regional Innovation System & Education (RISE) program through the Jeju RISE center, funded by MOE and the Jeju Special Self-Governing Province, Republic of Korea (2025-RISE-17-001).

COMPETING INTERESTS

The authors declare no competing interests.

ETHICS APPROVAL AND CONSENT TO PARTICIPATE

For animal studies, all experimental procedures were performed in accordance with protocols approved by the Institutional Animal Care and Use Committee of UNIST (UNISTACUC-20-27).

ADDITIONAL INFORMATION

Supplementary information The online version contains supplementary material available at <https://doi.org/10.1038/s41420-026-02978-3>.

Correspondence and requests for materials should be addressed to Hyug Moo Kwon or Soo Youn Choi.

Reprints and permission information is available at <http://www.nature.com/reprints>

Publisher's note Springer Nature remains neutral with regard to jurisdictional claims in published maps and institutional affiliations.



Open Access This article is licensed under a Creative Commons Attribution 4.0 International License, which permits use, sharing, adaptation, distribution and reproduction in any medium or format, as long as you give appropriate credit to the original author(s) and the source, provide a link to the Creative Commons licence, and indicate if changes were made. The images or other third party material in this article are included in the article's Creative Commons licence, unless indicated otherwise in a credit line to the material. If material is not included in the article's Creative Commons licence and your intended use is not permitted by statutory regulation or exceeds the permitted use, you will need to obtain permission directly from the copyright holder. To view a copy of this licence, visit <http://creativecommons.org/licenses/by/4.0/>.

© The Author(s) 2026